Published in Ain Shams Engineering Journal with doi: 10.1016/j.asej.2022.101872

Optimal Allocation of Renewable DGs Using Artificial Hummingbird Algorithm under Uncertainty Conditions

Ashraf Ramadan[1], Mohamed Ebeed[2], Salah Kamel[1], Emad M. Ahmed [3,*], Marcos Tostado-Véliz[4,*]

[1]Department of Electrical Engineering, Aswan University, Aswan 81542, Egypt; ashraframadanragab@gmail.com (A.R), skamel@aswu.edu.eg (S.K.)
[2]Faculty of Engineering, Sohag University, Sohag 82524, Egypt; mebeed@eng.sohag.edu.eg (M.E.).
[3]Department of Electrical Engineering, College of Engineering, Jouf University, Sakaka 72388, Saudi Arabia
[4] Department of Electrical Engineering, University of Jaén, Jaén, Spain
*Email: emamahmoud@ju.edu.sa (E.M.A.); mtostado@ujaen.es (M.T.-V.)

Abstract:

Renewable distributed generators (RDGs) have been widely used in distribution networks for technological, economic, and environmental reasons. The main concern with renewable-based distributed generators, particularly photovoltaic and wind systems, is their intermittent nature, which causes output power to fluctuate, increasing power system uncertainty. As a result, it's critical to think about the resource's uncertainty when deciding where it should go in the grid. The main innovation of this paper is proposing an efficient and the most recent technique for optimal sizing and placement of the RDGs in radial distribution systems considering the uncertainties of the loading and RDGs output powers. Monte-Carlo simulation approach and backward reduction algorithm are used to generate a reasonable number of scenarios to reflect the uncertainties of loading and RDG output power. The artificial hummingbird algorithm (AHA), which is considered the most recent and efficient technique, is used to estimate the RDG ratings and placements for a multi-objective function that includes minimizing expected total cost, total emissions, and total voltage deviation, as well as improving expected total voltage stability. The proposed technique is tested using an IEEE 33-bus network and an actual distribution system in Portugal (94-bus network). Simulations show that the suggested method effectively solves the problem of optimal DG allocation. Furthermore, the results show that using the proposed method to optimally integrate wind turbines with solar-based DG reduces expected costs, emissions, and voltage deviations while also improving voltage stability by 38.91 %, 62.43 %, 70.48 %, and 12.12 %, respectively, in the IEEE 33-bus system, while these values are improved by 39.6 %, 62.59 %, 78.52 %, and 23.24 %, respectively, in the 94-bus system.

Keywords: Uncertainties, Artificial hummingbird algorithm, Backward reduction algorithm, Monte-Carlo simulation, Renewable Energy, Wind, Solar.

1. Introduction

The desire to incorporate distributed generators (DGs) into radial distribution systems (RDSs) has developed in recent decades due to their technical, economic, and environmental benefits, which include increasing power grid efficiency, improving voltage profile and reducing power losses. If the integration of DGs is not correctly planned, however, technical concerns such as over-voltage, fluctuation, and system unbalance can arise. Furthermore, dealing with DG-based renewable energy resources, such as wind power and photovoltaic (PV), which are characterized by intermittent power generation in addition to load variation, resulted in an increase in the change in power losses and voltage level. The proper DG allocation (placement and size) into RDS is primarily required to minimize these challenges and improve the benefits of DG integration [1,2].

In recent years, installing distributed generation (DG) sources in distribution network systems has been normal practice to ensure that the distribution network's performance is optimal, in other words, to reduce total power losses and improve power quality [3,4]. The shift to increased renewable energy (RE) shares will make it easier to achieve universal access to clean, cheap electricity while also reducing the majority of global greenhouse gas (GHG) emissions. Renewable electricity is becoming more cost-competitive with traditional power facilities due to cost decreases [5]. Taking into account all uncertain parameters increases the model's complexity and computing weight, but it also results in a more accurate and efficient model. Input uncertainties and network uncertainties are two types of uncertainty in power systems. The input uncertainties are due to stochastic load demand and power generation randomization. A backward reduction approach was employed to reduce the amount of scenarios formed by Monte Carlo simulations [6,7]. The benefits of optimal DG allocation and optimal planning include lower energy prices, lower emissions, and improved voltage profiles and power quality [8–10]. However, because RERs are generally uncertain, incorrect DG placement can result in voltage fluctuations and system instability [11,12]. A lot of research have made an analysis of optimal DG integration from numerous perspectives. The authors of [13] examines several technological challenges related to the stability issues associated with extensive PV penetration into the power grid. Frequency regulation, active power reduction, reactive power injection, and storing energy are only a few examples. In [14], the ramp-rate (RR) control algorithms have been used with Energy Storage Systems (ESS) for minimizing the power fluctuations to the grid. In [15], the technical challenges, such as frequency disturbances and voltage limit violation, that arise as a result of the large-scale and intensive PV system penetration into the power network, as well as the stability issues that result. The impact of large-scale PV system integration on the grid is also considered, as well as possible solutions. In [16], a solution called search-based dragonfly algorithm (DFA) was presented for optimal allocation of the DGs considering the load and DGs uncertainties. In [17], an evaluation of the best strategies for sizing and locating distributed generation in distribution networks. The Artificial Hummingbird Algorithm (AHA) is a new and effective bio-inspired algorithm [18]. In this research, the AHA is used to identify the optimal solar / wind unit allocation in IEEE 33-bus and 94-bus networks to minimize expected total voltage deviation, cost, emissions, and improving expected total stability of voltage, considering uncertainties of load demands, solar, and wind power generators. The contributions and innovation of this paper are summarized as follows:

- Application of an efficient and the most recent technique called the AHA for assigning the optimal location and sizes of the RDGs.
- The allocation problem of the RDGs is solved under uncertainties of the loading and the output powers of the RDGs.
- The uncertainties of system are addressed using the Monte-Carlo simulation method along with the backward reduction algorithm.
- The allocation problem of the RDGs is solved for the total cost, the total emissions, voltage improvements, system voltage deviation, of the IEEE 33-bus and an actual distribution system in Portugal 94-bus network.
- The AHA is evaluated in comparison to a number of well-known problem-solving algorithms.

The following is a summary of the structure of the paper: Section II shows the problem formulation, which contains the objective function. In Section III, we'll look at how to model uncertainty. The IV section provides an overview of the AHA approach. Section V shows the collected data, whereas Section VI summarizes the paper's results.

2. PROBLEM FORMULATION

This research proposes a multi-objective function; four objective functions are examined. It's worth mentioning that many scenarios must be addressed when modeling or estimating power system uncertainty

2.1. Objective functions

2.1.1 MINIMIZE EXPECTED TOTAL COST (ETCOST)

Expected total annual cost ($\boldsymbol{ETCost}$) is taken into account, which contains the expected cost of the electric substation ($\boldsymbol{ECost_{Grid}}$), the PV units cost expected ($\boldsymbol{ECost_{PV}}$) and WT cost expected ($\boldsymbol{ECost_{WT}}$), and can be expressed in the following way:

$$\boldsymbol{ETCost} = \boldsymbol{ECost_{Grid}} + \boldsymbol{ECost_{PV}} + \boldsymbol{ECost_{WT}} \tag{1}$$

where $\boldsymbol{ETCost}$ is denotes the total cost expected.

The following are the main items of Eq. (1):

$$ETCost_{Grid} = \sum_{k=1}^{Ns} ECost_{Grid,k} = \sum_{k=1}^{Ns} Cost_{Grid,k} \times \pi_{S,k} \tag{2}$$

$$Cost_{Grid} = P_{Grid} \times K_{Grid} \tag{3}$$

$$ETCost_{PV} = \sum_{k=1}^{Ns} ECost_{PV,k} = \sum_{k=1}^{Ns} \pi_{Solar,k} \times (a_{PV} + b_{PV} * PG_{PV}) \tag{4}$$

$$a_{PV} = \frac{capital\ cost\_PV * P_{sr} * Gr}{life\ time\_PV * 8760 * LF} \tag{5}$$

$$b_{PV} = Cost\_PV_{O\&M} + Cost\_PV_{Fuel} \tag{6}$$

$$ETCost_{wind} = \sum_{k=1}^{Ns} ECost_{wind,k} = \sum_{k=1}^{Ns} \pi_{wind,k} \times (a_{wind} + b_{wind} * PG_{wind}) \tag{7}$$

$$a_{wind} = \frac{capital\ cost\_wind * P_{wr} * Gr}{life\ time\_wind * 8760 * LF} \tag{8}$$

$$b_{wind} = Cost\_wind_{O\&M} + Cost\_wind_{Fuel} \tag{9}$$

where a_{PV} is the cost of installing a PV unit on an annual basis, and b_{PV} the annual cost of operating and maintaining of a PV unit. The installing cost of a WT unit on an annual basis is a_{wind}, annual cost of WT Operating and Maintenance cost is b_{wind}, annual rate of benefit (\$/h) is Gr, load factor of DGs is LF, and K_{Grid} = 0.096 [19].

2.1.2 MINIMIZE THE EXPECTED TOTAL EMISSIONS ($ETEmission$)

The following is an estimate of total annual emissions in kilotons: Emissions reduction from generation units (f2): CO2, SO2, and NOx are the most effective pollutants in power generation sources. This objective function's mathematical formulation is as follows [19]:

$$\boldsymbol{ETEmission} = \sum_{k=1}^{Ns} \boldsymbol{EEmission_k} = \sum_{k=1}^{Ns} \boldsymbol{\pi_{Grid,k}} \times \boldsymbol{E_{Grid,k}} \tag{10}$$

$$\boldsymbol{f_2(x)} = \sum_{i=1}^{N_{DG}} \boldsymbol{E_{DG_i}} + \boldsymbol{E_{Grid}} \tag{11}$$

$$\boldsymbol{E_{DG_i}} = (\boldsymbol{CO_2^{DG}} + \boldsymbol{NO_x^{DG}} + \boldsymbol{SO_2^{DG}}) \times \boldsymbol{PG_i} \tag{12}$$

$$\boldsymbol{E_{Grid}} = (\boldsymbol{CO_2^{Grid}} + \boldsymbol{NO_x^{Grid}} + \boldsymbol{SO_2^{Grid}}) \times \boldsymbol{P_{gGrid}} \tag{13}$$

where $\boldsymbol{ETEmission}$ is the expected total emission[19].

2.1.3 MINIMIZE EXPECTED VOLTAGE DEVIATIONS (EVD)

The summation voltage expected deviations of the RDN is identified as follows:

$$\boldsymbol{ETVD} = \sum_{L=1}^{Ns} \boldsymbol{EVD_L} = \sum_{L=1}^{Ns} \boldsymbol{\pi_{S,L}} \times \boldsymbol{VD_L} \tag{14}$$

where:

$\boldsymbol{ETVD}$ is refers to the total voltage expected deviations

$$\boldsymbol{VD} = \sum_{k=1}^{n} |\boldsymbol{V_k} - \mathbf{1}| \tag{15}$$

2.1.4 ENHANCEMENT EXPECTED TOTAL VOLTAGE STABILITY INDEX (ETVSI)

$$\boldsymbol{ETVSI} = \sum_{L=1}^{Ns} \boldsymbol{EVSI_L} = \sum_{L=1}^{Ns} \boldsymbol{\pi_{S,L}} \times \boldsymbol{VSI_L} \tag{16}$$

where $\boldsymbol{ETVSI}$ is denotes the expected total voltage stability index

$$\boldsymbol{VSI_n} = |\boldsymbol{V_n}|^4 - 4(\boldsymbol{P_n X_{nm}} - \boldsymbol{Q_n R_{nm}})^2 - 4(\boldsymbol{P_n X_{nm}} + \boldsymbol{Q_n R_{nm}})|\boldsymbol{V_n}|^2 \tag{17}$$

2.1.5 THE MULTI-OBJECTIVE FUNCTION

This research shows preceding objective functions are taken into account at the same time. The weight approach method is utilized to take into account several goal functions at the same time. The objective function is described in the following way:

$$\boldsymbol{F} = \Omega_1 \boldsymbol{F_1} + \Omega_2 \boldsymbol{F_2} + \Omega_3 \boldsymbol{F_3} + \Omega_4 \boldsymbol{F_4} \tag{18}$$

Ω_1, Ω_2, Ω_3 ,and $\Omega_4$are the weighing factors. As follows, the weight factors must accumulate to one:

$$|\Omega_1| + |\Omega_2| + |\Omega_3| + |\Omega_4| = \boldsymbol{1} \tag{19}$$

The following is a formula for normalized objective functions:

$$F_1 = \frac{ETCost}{ETCost_{base}} \tag{20}$$

$$\boldsymbol{F_2} = \frac{\boldsymbol{ETEmission}}{\boldsymbol{ETEmission_{base}}} \tag{21}$$

$$\boldsymbol{F_3} = \frac{\boldsymbol{ETVD}}{\boldsymbol{ETVD_{base}}} \tag{22}$$

$$\boldsymbol{F_4} = \frac{\boldsymbol{1}}{\boldsymbol{ETVSI}} \tag{23}$$

2.2 Constraints of the System

The following are the categories of system constraints:

2.2.1 EQUALITY CONSTRAINTS

$$\boldsymbol{P_{Grid}} + \sum_{j=1}^{NPV} \boldsymbol{P_{PV,j}} + \sum_{j=1}^{NWT} \boldsymbol{P_{WT,j}} = \sum_{j=1}^{NT} \boldsymbol{P_{loss,j}} + \sum_{j=1}^{NB} \boldsymbol{P_{L,j}} \tag{24}$$

$$\boldsymbol{Q_{Grid}} + \sum_{j=1}^{NT} \boldsymbol{Q_{WT,j}} = \sum_{j=1}^{NT} \boldsymbol{Q_{loss,j}} + \sum_{j=1}^{NB} \boldsymbol{Q_{L,j}} \tag{25}$$

2.2.2 INEQUALITY CONSTRAINTS

$$V_{min} \leq V_j \leq V_{max} \tag{26}$$

$$\sum_{j=1}^{NWT} Q_{WT,j} \leq \sum_{j=1}^{NB} Q_{L,j} \tag{27}$$

$$I_n \leq I_{max,n} \quad n = 1,2,3 \ldots, NT \tag{28}$$

3. Uncertainty Modeling of WT, PV Unit, and Load Demand.

3.1 Wind DG Uncertainty Modeling

The Weibull PDF was used in modeling wind speed uncertainty [20]:

$$f_v(v) = \left(\frac{\beta}{\alpha}\right) \left(\frac{v}{\alpha}\right)^{(\beta-1)} \exp\left[-\left(\frac{v}{\alpha}\right)^{\beta}\right] \; 0 \leq v < \infty \tag{29}$$

Weibull PDF's scaling and shaping factors are α, β. Figure 1 shows a 1000 Monte-Carlo wind speed distribution scenario using Weibull PDF.

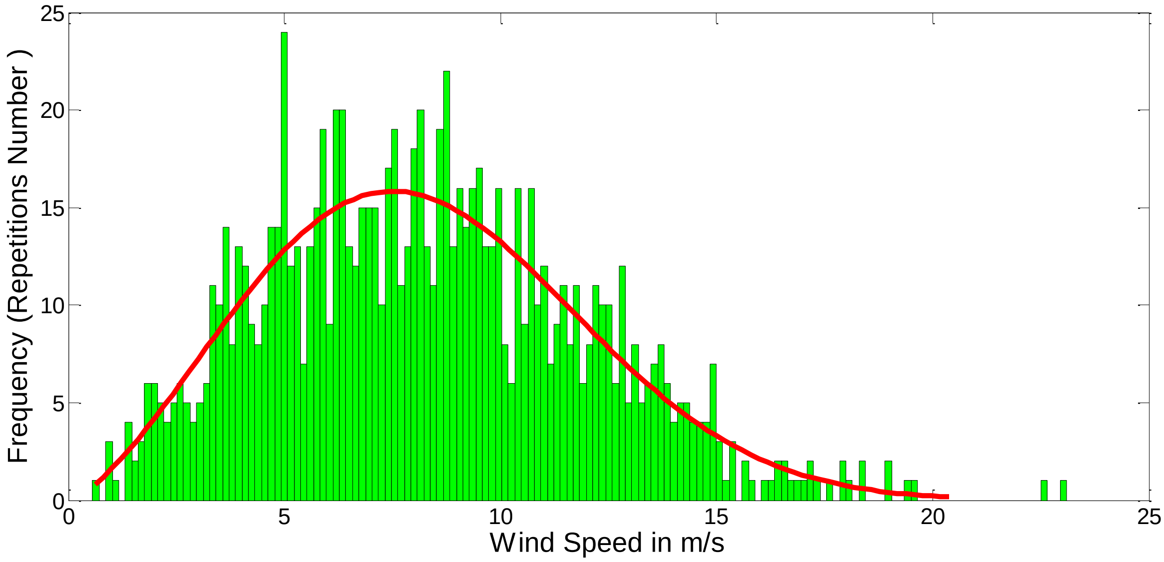

FIGURE 1. Applying Weibull PDF at (α = 9.3, β = 2.3).

The output power of a WT can be expressed as a function of wind speed. [20]:

$$P_\omega(v_\omega) = \begin{cases} 0 & for \quad v_\omega < v_{\omega i}\, v_\omega > v_\omega \\ P_{\omega r}\left(\dfrac{v_\omega - v_{\omega i}}{v_{\omega r} - v_{\omega i}}\right) & for \quad (v_{\omega i} \le v_\omega \le v_{\omega r}) \\ P_{\omega r} & for \quad (v_{\omega r} \le v_\omega \le v_{\omega o}) \end{cases} \tag{30}$$

where, $P_{\omega r}$ is the rated output power of the WT, $v_{\omega i}$ =3 m/s , $v_{\omega o}$=25 m/s and $v_{\omega r}$ =16 m/s, are the cut-in, cut-out, and rated speed of WT, respectively.

The probability of wind speed is calculated for each wind scenario using (31).

$$\tau_{wind,K} = \int_{v_K^{min}}^{v_K^{max}} f_v(v) \ dv \tag{31}$$

where, $\tau_{wind,K}$ is the WT probability in the K scenario and v_K^{min}, v_K^{max} is the limits of wind speed at $K^{\ th}$scenario.

3.2 Solar DG uncertainty Modeling

The lognormal PDF can be used to express the uncertainty in solar irradiation [21]:

$$f_H(H) = \frac{1}{H\ \sigma_s\sqrt{2\pi}} \quad exp\left[-\frac{(\ln H - \mu_s)^2}{2{\sigma_s}^2}\right] \quad for\ H\ > 0 \tag{32}$$

As, $\mu_{s,}$ / σ_s, are the mean / standard deviation of the random variables that have been set to be equal to 5.4 and 0.4, respectively[21].

Figure 2 depicts the solar irradiation scenarios generated by the Monte-Carlo simulation.

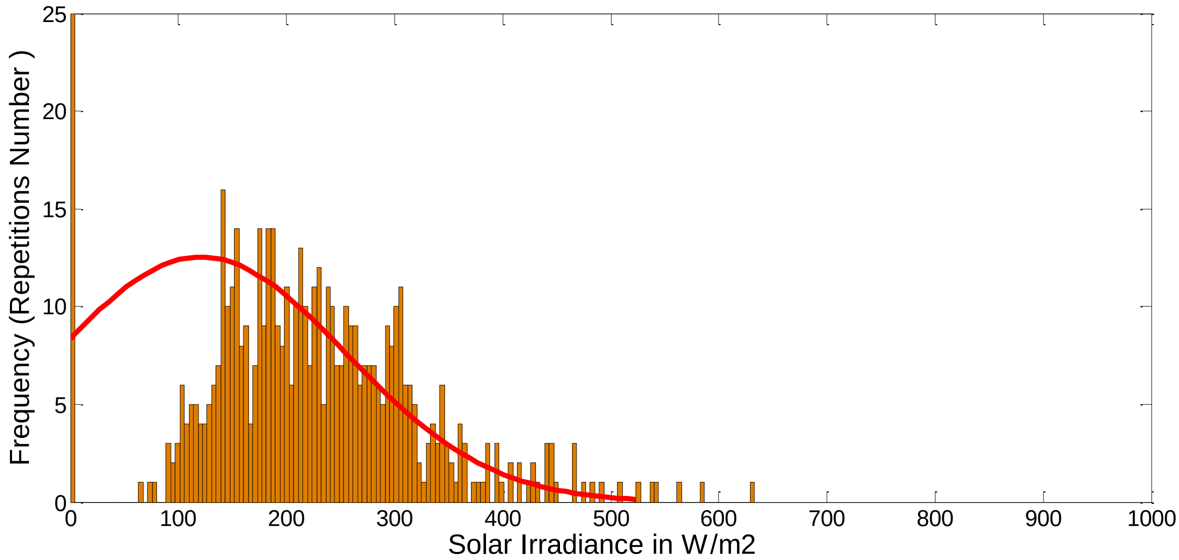

FIGURE 2. PV unit solar irradiation scenarios.

The following formula can be used to compute the PV array output power as a function of irradiance [21]:

$$P_s(H) = \begin{cases} P_{sr}\left(\frac{H^2}{H_{std}\ \times\ M_c}\right) & for\quad 0 < \quad H \quad \leq \quad M_c \\ P_{sr}\left(\frac{H}{H_{std}}\right) & for \quad H \quad \geq \quad M_c \end{cases} \tag{33}$$

where, H_{std} is the sun's standard irradiation, which is 1000 W/m2, and M_c is a certain point of irradiance equal 120 W/m2 [21].

The probability of solar irradiation could be calculated using [21]:

$$\tau_{solar,m} = \int_{H_n^{min}}^{H_n^{max}} f_H(H) \;\; dH \tag{34}$$

As, H_n^{min} and H_n^{max} are the limits of solar irradiance's interval at n-th scenario

3.2 Load Demand Uncertainty Modeling

The normal distribution PDF can be used in load modeling [22]:

$$f_d(P_d) = \frac{1}{\sigma_d\sqrt{2\pi}} \;\; exp\left[-\frac{(P_d - \mu_d)^2}{2{\sigma_d}^2}\right] \tag{35}$$

where, σ_d and μ_d, are the standard and mean deviation values respectively. P_d signifies the probability density of the load normal distribution. Figure 3 shows load demand Monte Carlo simulations molded with a normal distribution [22]:

$$\tau_{d,i} = \int_{v_{d,i}^{min}}^{v_{d,i}^{max}} \frac{1}{\sigma_d\sqrt{2\pi}} \;\; exp\left[-\frac{(P_d - \mu_d)^2}{2{\sigma_d}^2}\right] \;\; dp_d \tag{36}$$

$$P_{d,i} = \frac{1}{\tau_{d,i}} \int_{P_{d,i}^{min}}^{P_{d,i}^{max}} \frac{P_d}{\sigma_d\sqrt{2\pi}} \;\; exp\left[-\frac{(P_d - \mu_d)^2}{2{\sigma_d}^2}\right] \;\; dp_d \tag{37}$$

where, $P_{d,i}^{min}, P_{d,i}^{max}$ reflect the $i - th$ interval's boundaries

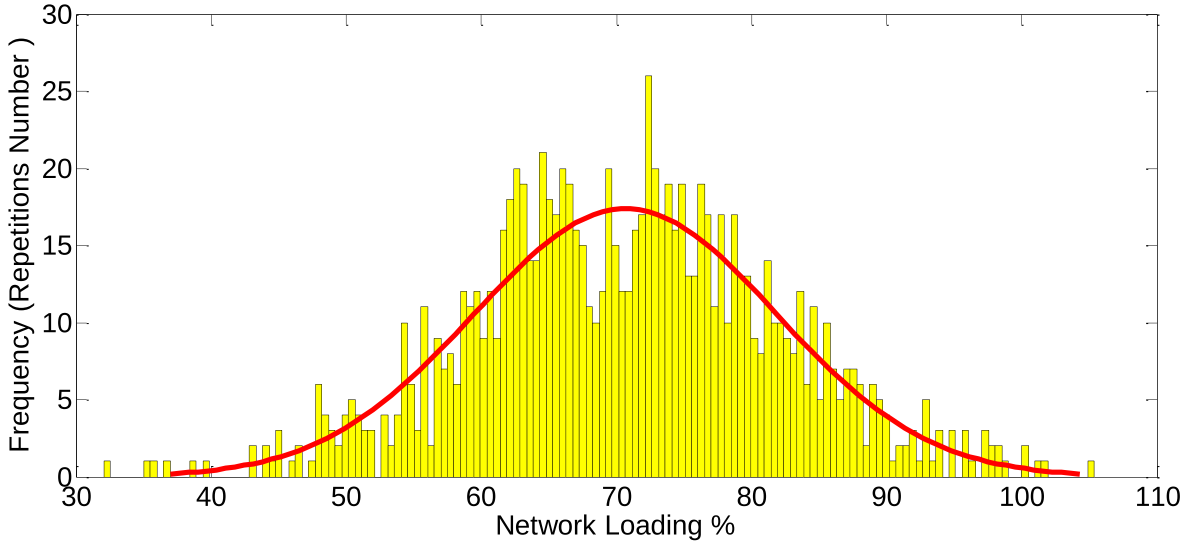

FIGURE 3. Applying normal PDF at (σ_d= 11 , μ_d = 71)

E. Backward Reduction Algorithm

Ref. [23] explains how to limit possibilities by using the backward reduction technique (BRA). Table 1 shows the probabilities associated with the various example scenarios.

Each row of this table shows each scenario probability, as well as loading, wind speed, and solar irradiance.

Table 1. Selected scenarios, as well as the associated uncertainties

Scenario	Loading %	Wind speed (m/s)	Solar irradiance (W/m2)	π_S
$S1$	84.25477	4.674154	585.4496	0.001
$S2$	66.14756	12.19066	92.35944	0.009
$S3$	75.2173	12.09984	280.9624	0.13
$S4$	69.55373	9.977456	0	0.485
$S5$	104.46	8.340612	195.1718	0.002
$S6$	67.81934	9.448742	203.8083	0.149
$S7$	76.93514	5.920562	539.0844	0.005
$S8$	67.83325	5.812723	128.3179	0.062
$S9$	75.22243	3.409302	444.9522	0.017
$S10$	64.98827	4.673502	632.9788	0.001
$S11$	75.91118	8.597734	164.0013	0.091
$S12$	65.94618	9.12221	364.0274	0.048

4. OPTIMIZATION ALGORITHMS

The Artificial Hummingbird Algorithm (AHA) is the most recent bio-inspired optimization technique for solving engineering applications, which was introduced around the end of 2021. It is based on the intelligent behaviors of hummingbirds. **[18].** The AHA is comparable to other optimization techniques that create the exploration and exploitation stages. Three components, including Food sources, Hummingbirds, and Visit table, describe the development for solving different optimization challenges. Hummingbirds evaluate the features of sources in general, for example, the content and nectar quality of exact flowers, the rate at which nectar is produced, and the last time they visited the flower. Hummingbirds can remember the location and pace of nectar replenishment of a single food source and pass this information on to other hummingbirds in the community. The number of hummingbirds that visit each food source is recorded in the hummingbird visits table. During each loop, the visit table is generally updated. The development is determined by three foraging techniques: directed, territorial, and migrating foraging. Below are the mathematical models for the three foraging methods.

4.1 Initialization

As follows, a population of n hummingbirds is randomly placed on n food sources. [18]:

$$x_i = Low + r * (Up - Low) \quad i = 1, \dots, n \tag{38}$$

where Low and Up are the lower and upper limits, respectively, x_i denotes the position of the ith food source it is the solution to a specific problem, r is a random vector in [0, 1], and The initialization of the visit table of food sources is as follows.:

$$VT_{i,j} = \begin{cases} 0 & if \quad i \neq j \\ null & i = j \end{cases} \qquad i = 1, \dots, n;\ j = 1, \dots, n \tag{39}$$

As for $i = j$, $VT_{i,j}$ = null illustrates that a hummingbird is consuming food from a specific source; the ith hummingbird has just visited the food source, for $i \neq j$, $VT_{i,j}$ = 0 displays that the jth in the current iteration.

4. 2. Guided foraging

Each hummingbird proceeds to the nectar source that has the most nectar. Hummingbirds fly in three different ways: axial flight, diagonal flight, and omnidirectional flight. The following is the definition of axial flight:

$$D^{(i)} = \begin{cases} 1 & if \quad i = randi([1, d]) \\ 0 & else \end{cases} \qquad i = 1, \dots, d \tag{40}$$

The following is a definition of diagonal flight:

(41)

$$D^{(i)} = \begin{cases} 1 & if \quad i = P(j), j \in [1,k], P = randperm(k), k \in [2, \lceil r_1 * (d-2) \rceil + 1] \\ 0 & else \end{cases} \quad i = 1, \dots ,$$

The following is the definition of omnidirectional flight:

$$D^{(i)} = 1 \qquad i = 1, \dots , d \tag{42}$$

where, $randperm(k)$ builds a number permutation from 1 to k and $randi\ [1, d]$ generates a number at random between 1 and d, and $r1$ is a random number (0, 1]. The following is the mathematical equation for modeling directed foraging behavior with an appropriate food source:

$$v_i(t+1) = x_{i,tar}(t) + a * D * (x_i(t) - x_{i,tar}(t)) \tag{43}$$

$$a \sim N\ (0,1) \tag{44}$$

where, the position of the $\boldsymbol{ith}$ hummingbird's intended food source is $\boldsymbol{x_{i,tar}}$ (t) and $\boldsymbol{a}$ is a guided factor, at the normal distribution $\boldsymbol{N(0,1)}$ with standard deviation = 1 and mean = 0, and $\boldsymbol{x_i(t)}$ is the location of the $\boldsymbol{ith}$ food source at time $\boldsymbol{t}$.

The following is the latest position update for the $\boldsymbol{ith}$ food source:

$$x_i(t+1) = \begin{cases} x_i(t) & f(x_i(t)) \le f(v_i(t+1)) \\ v_i(t+1) & f(x_i(t)) > f(v_i(t+1)) \end{cases} \tag{45}$$

If the candidate food source's nectar-refilling rate is higher than the current food source, the hummingbird cancels the current food source and feeds at the candidate food source determined by Eq. (43) instead, according to Eq. (45).

4. 3. Territorial foraging

Inside its own region, a hummingbird can easily move to a nearby position, where it can locate a new food supply that is potentially better than the one it now has.

Hummingbirds' local foraging strategy and a suitable food source in their territorial foraging strategy are described by the mathematical equation below:

$$v_i(t+1) = x_i(t) + b * D * x_i(t) \tag{46}$$

$$b \sim N\ (0,1) \tag{47}$$

where $\boldsymbol{b}$ is a territorial factor with a mean of 0 and a standard deviation of 1 and is subject to the normal distribution $\boldsymbol{N}\ (\mathbf{0}, \mathbf{1})$. Using its specific flight talents.

4. 4. Migration foraging

The migration of a hummingbird from the lowest nectar refilling rate nectar source to a new one generated at random can be described as follows:

$$x_{wor}(t+1) = Low + r * (Up - Low) \tag{48}$$

where $\boldsymbol{x_{wor}}$ is the food with the lowest rate of nectar replenishment in the population

A hummingbird practicing directed foraging and territorial foraging would visit each food source in turn as its target source according to the visit table at each iteration if there is no replacement for all food sources. Assume that choosing between guided and territorial foraging has a 50% chance of success, and that in guided foraging, visiting every other source has a 50% chance of success. In this case, a migratory foraging approach must be used to alleviate stasis and broaden the search area. As a result, the following population size specification for the migration co-efficient is proposed:

$$M = 2n \tag{49}$$

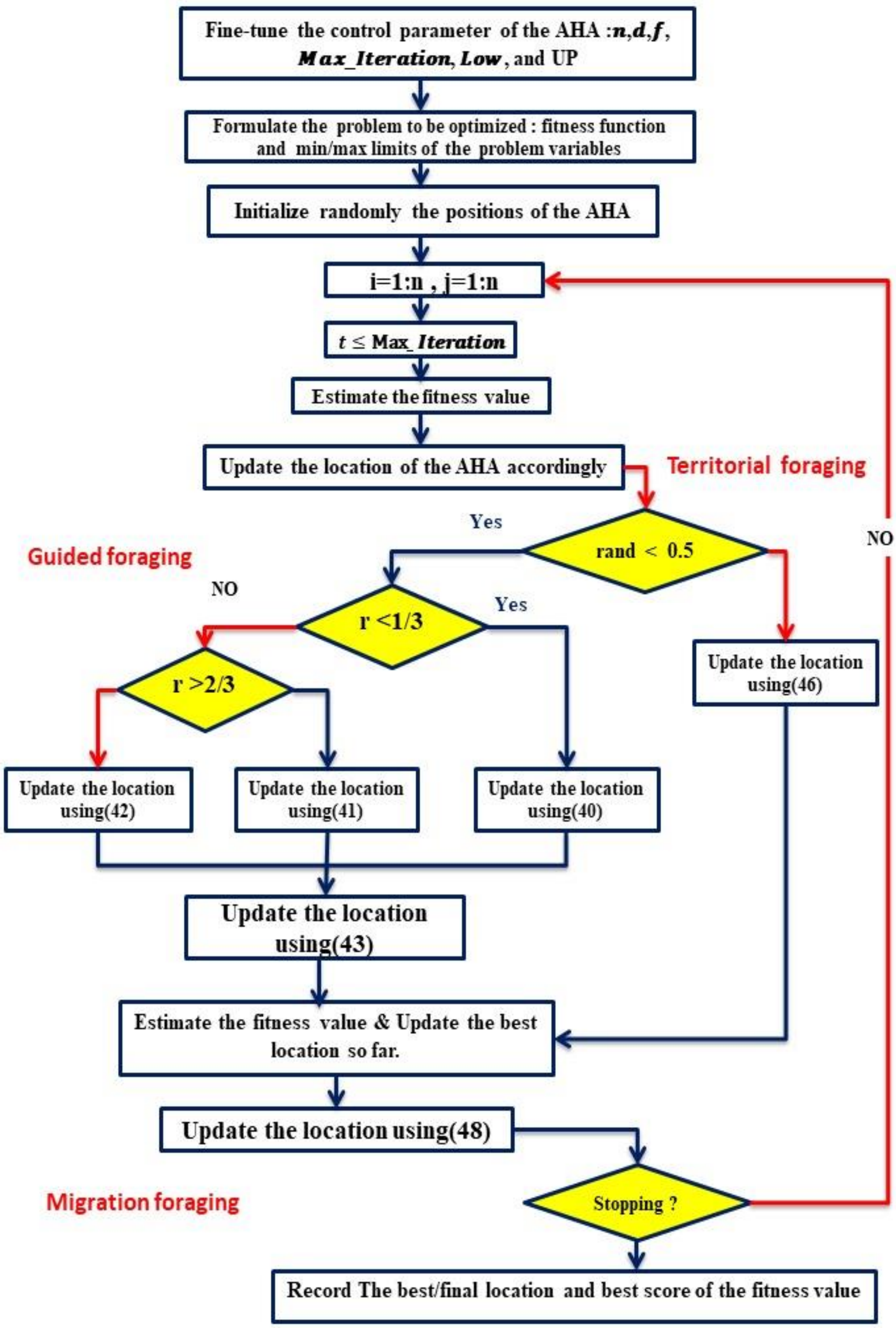

Figure 4. The AHA's flowchart.

5. SIMULATION RESULTS, DISCUSSION, AND COMPARISON

The proposed approach is used in this section to select the optimal RDGs allocations in two RDNs (IEEE 33-bus and 94-bus system) considering the system uncertainty by applying the AHA. These systems single line diagrams are depicted in Figures 5 and 6. The branches and buses of the IEEE 33-bus and 94-bus systems are defined in [24] and [25], respectively. Table 2 depicts the specification of the studied networks. The information gathered was compared to well-known optimization algorithms to verify the effectiveness of the proposed algorithm such as Whale Optimization Algorithm (WOA), Ant Lion Optimizer (ALO), Particle Swarm Optimizer (PSO), and Sine Cosine Algorithm (SCA). Table 3 shows the parameters of several techniques, whereas Table 4 shows the system's limitations. The characteristics of the generation resources are shown in Table 5. The proposed techniques for solving the allocation problem were designed in MATLAB 2014a on a Personal Computer with a 16 GB RAM and 3.2 GHz CPU and. The studied cases are:

Table 2. The specification of the studied networks.

Item	IEEE 33-bus	94-bus
System voltage	12.66 KV	15KV
Minimum voltage (p.u)	0.90378 @ bus 18	0.84749 @ bus 92
Maximum voltage (p.u)excluding the slack bus	0.99703 @ bus 2	0.99508 @ bus 2
Total active load demand (KW)	3715.000	4797.000
Total reactive load demand (KVAR)	2300.000	2323.900
Total Reactive Loss (KVAR)	143.022	505.785
Total Active Loss (KW)	210.982	365.173

Table 3. The used Parameters**.**

Optimizer	Configuration Parameters
AHA	T_{max} = 100, populations = 25.
WOA	T_{max} = 100, populations = 25.
ALO	T_{max} = 100, populations = 25.
PSO	T_{max} = 100, populations = 25.
SCA	T_{max} = 100, populations = 25.

Table 4. System's Limit.

Parameter	limit
Voltage limits	$0.90 \leq V_i \leq 1.05$ p.u
limits of DGs size	$0 \leq P_{WT,PV} \leq P_L$ kW
limits of Power factor	$0.65 \leq PF_i \leq 1$

Table 5. Generating Resources Characteristics.

DG Type	Capital Cost ($/kw)	Life time (year)	O&M Cost ($/kwh)	Fuel Cost ($/kwh)	Rated Capacity (MW)	Emission Factors (lb/MWh)		
						NO_X	SO_2	CO_2
PV	3985	20	0.01207	-	1	-	-	-
WT	1822	20	0.00952	-	5	-	-	-
Grid	-	25	-	0.044	25	5.06	11.6	2031

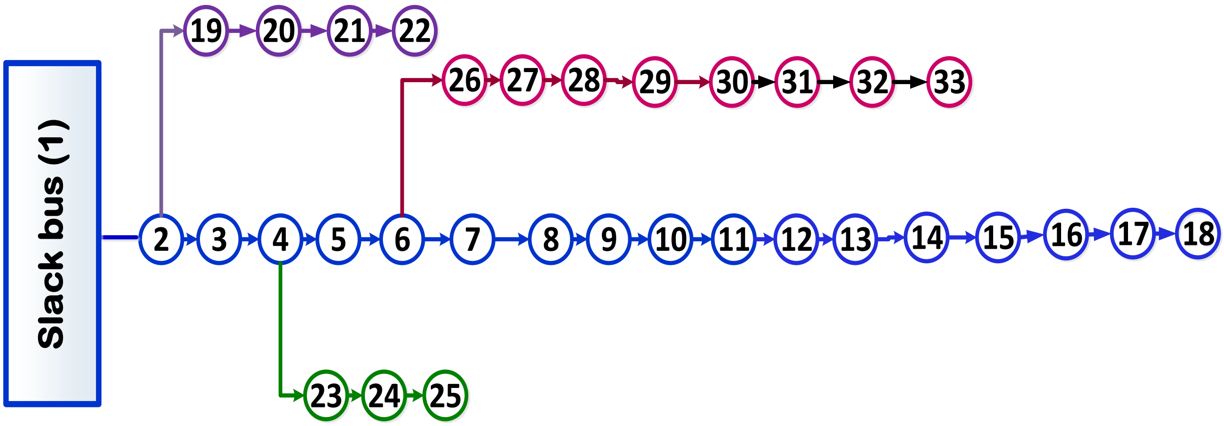

Figure 5. The topology of IEEE 33-bus system.

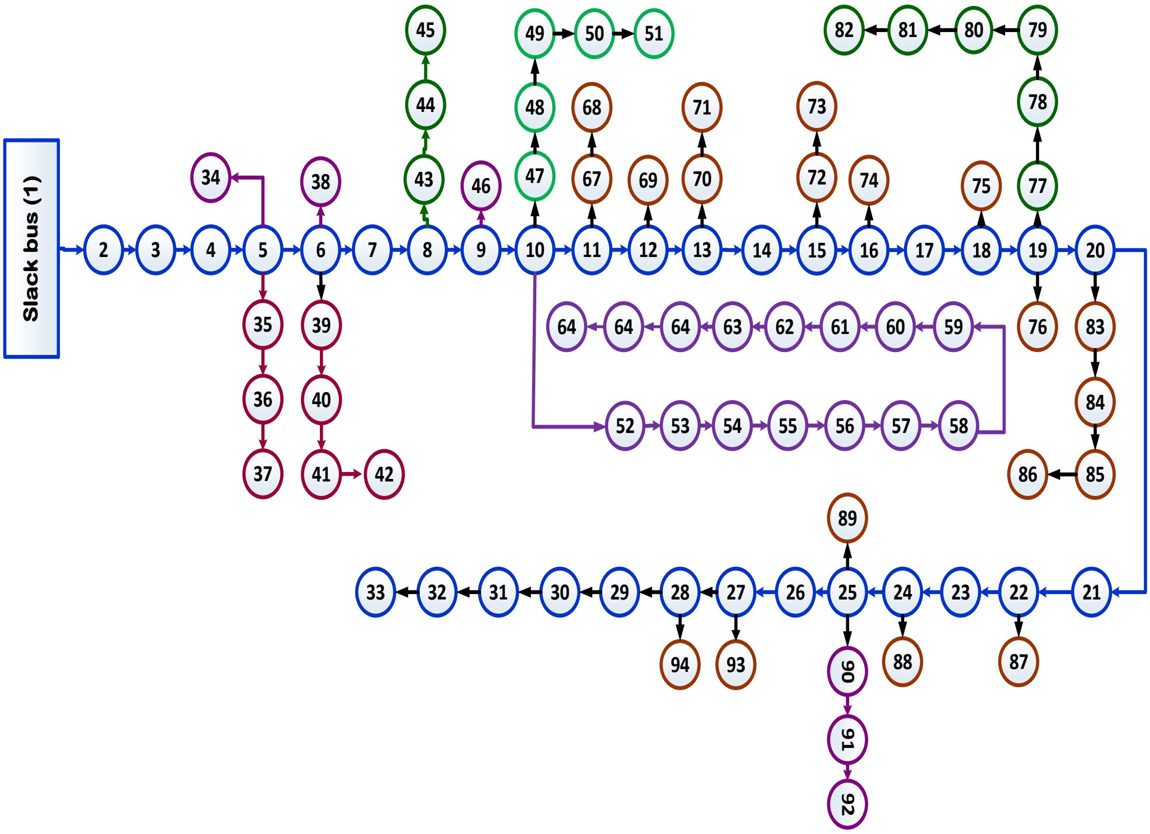

FIGURE 2. The topology of the 94-bus system.

5.1. THE IEEE 33-BUS SYSTEM

In this section, AHA is used to find the optimal RDGs sizing and siting in the IEEE 33-bus system. The results show that buses 14th and 7th are the best locations for PV / WT units, respectively. Distributed Generators sizes are 646kW and 3053kW, respectively. Table 6 shows the status of the distribution network with and without the inclusion of DGs. Because of differences in RDG output powers and load demand, the numbers in Table 7 change in each case. Figures 7, 8, 9, and 10 demonstrate the costs, emissions, voltage deviations, and voltage stability index for each scenario with and without RDG insertion, respectively. With the inclusion of the RDGs, the voltage deviation, emissions, and costs are all decreased significantly, while the VSI is significantly increased in each scenario. Figures 11 and 12 also show the voltage profiles of the IEEE 33-bus system in each scenario. The outputs of the objective function utilizing several optimization algorithms are shown in Table 8, and the AHA is superior to the PSO, WOA, SCA, and ALO strategies for resolving this issue.

Table 6. IEEE 33-bus system Simulation Results**.**

Item	Without RDGs	With RDGs	Percentage
Cost	264.4585	161.5546	38.91 %
Emmissin	5640800	2119500	62.43 %
VD	1.4141	0.4174	70.48 %
VSI	26.8151	30.5142	12.12 %

Table 7. The simulation results of IEEE 33-bus system.

Scenario	π_S	Loading %	$P_w(kW)$	$P_s(kW)$	$ETCost$(USD /h)	$ETEmission$ (kg/MWh)	$ETVD$(pu)	$ETVSI$(pu)
S1	0.001	84.25477	393.2	378.2004	0.29	5020	0.0011	0.028
S2	0.009	66.14756	2158.4	45.9213	0.8728	5650	0.0018	0.2881
S3	0.13	75.2173	2137.1	181.5017	15.5699	140830	0.0265	4.1484
S4	0.485	69.55373	1638.6	0	76.2319	984180	0.1875	14.8117
S5	0.002	104.46	1254.2	26.0810	0.617	10600	0.0019	0.0568
S6	0.149	67.81934	1514.5	131.6602	22.3736	278750	0.0516	4.5722
S7	0.005	76.93514	685.9	348.2485	1.1918	19320	0.004	0.1447
S8	0.062	67.83325	660.6	82.8934	14.3016	233990	0.0554	1.7743
S9	0.017	75.22243	96.1	287.4391	4.9774	87740	0.0204	0.4682
S10	0.001	64.98827	393	408.9043	0.2163	3440	0.0008	0.029
S11	0.091	75.91118	1314.6	105.9448	18.1373	269940	0.0521	2.7111
S12	0.048	65.94618	1437.8	235.1617	6.775	80040	0.0143	1.4817
Summation	**1**				**161.5546**	**2119500**	**0.4174**	**30.5142**

Table 8. The outcomes of using multiple Optimization techniques in the IEEE 33-bus system.

Optimizer	Average Values	Best Values	Worst Values	SD
AHA	**0.6237**	**0.6019**	**0.6564**	**0.0144**
PSO	0.7148	0.6096	0.9069	0.0646
ALO	0.6985	0.6087	0.7632	0.0446
WOA	0.6567	0.6047	0.7201	0.0336
SCA	0.6301	0.6112	0.6524	0.0118

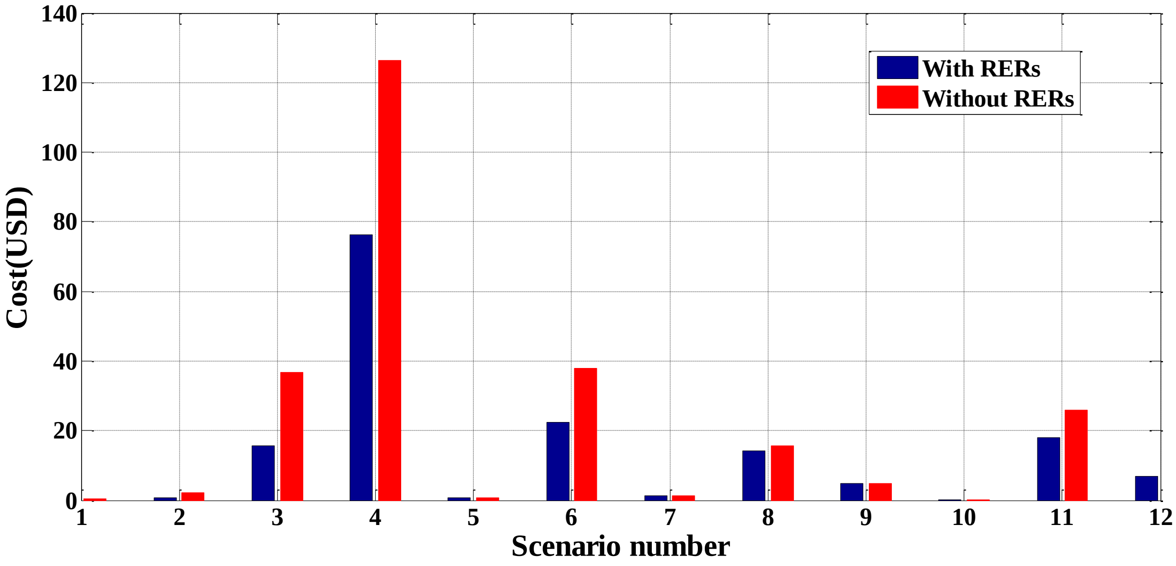

Figure 7. The total costs of IEEE 33-bus system.

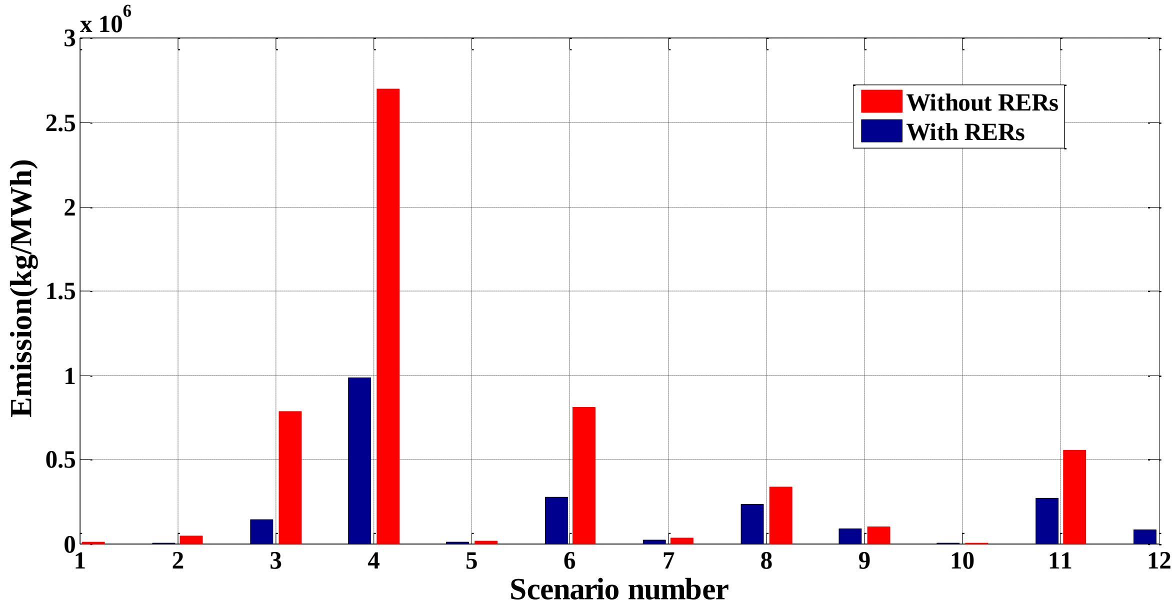

Figure 8. The total emissions of IEEE 33-bus system.

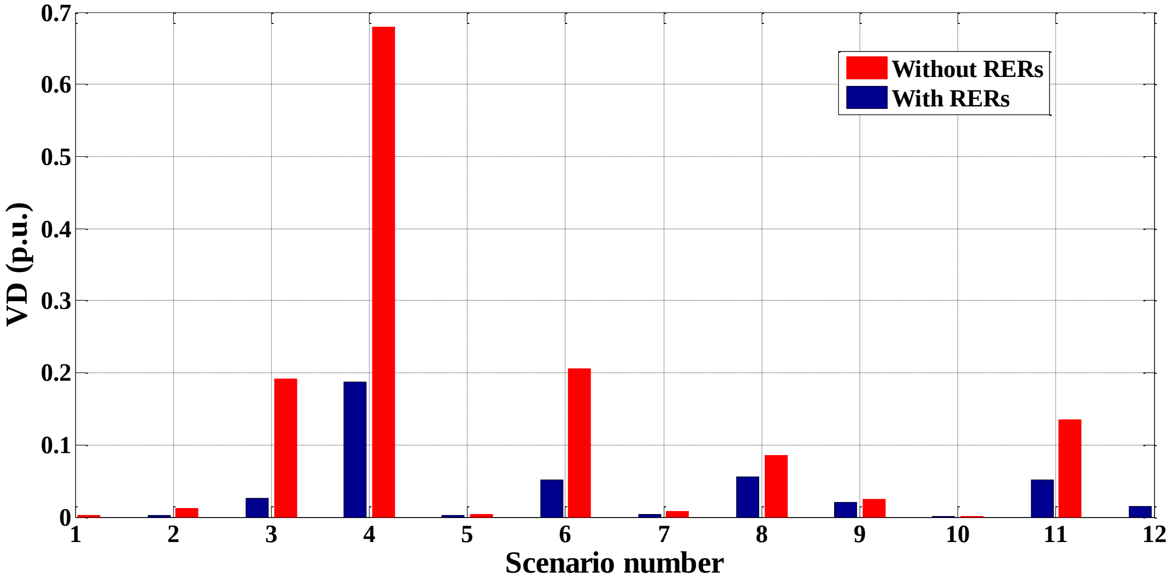

Figure 9. The total voltage deviations of IEEE 33-bus system.

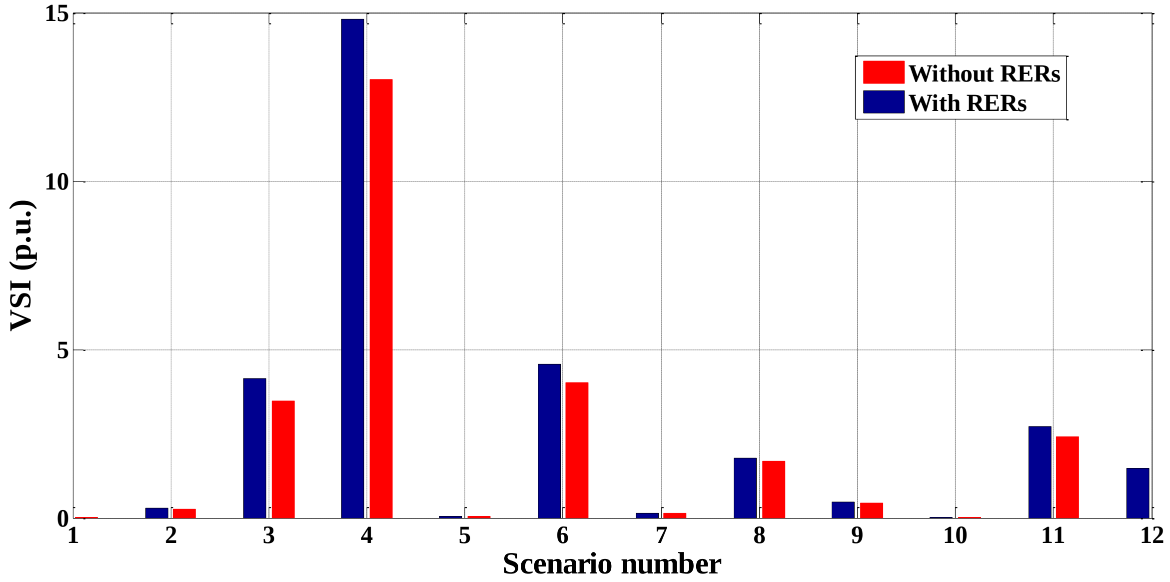

Figure 10. The total voltage stability index of IEEE 33-bus system.

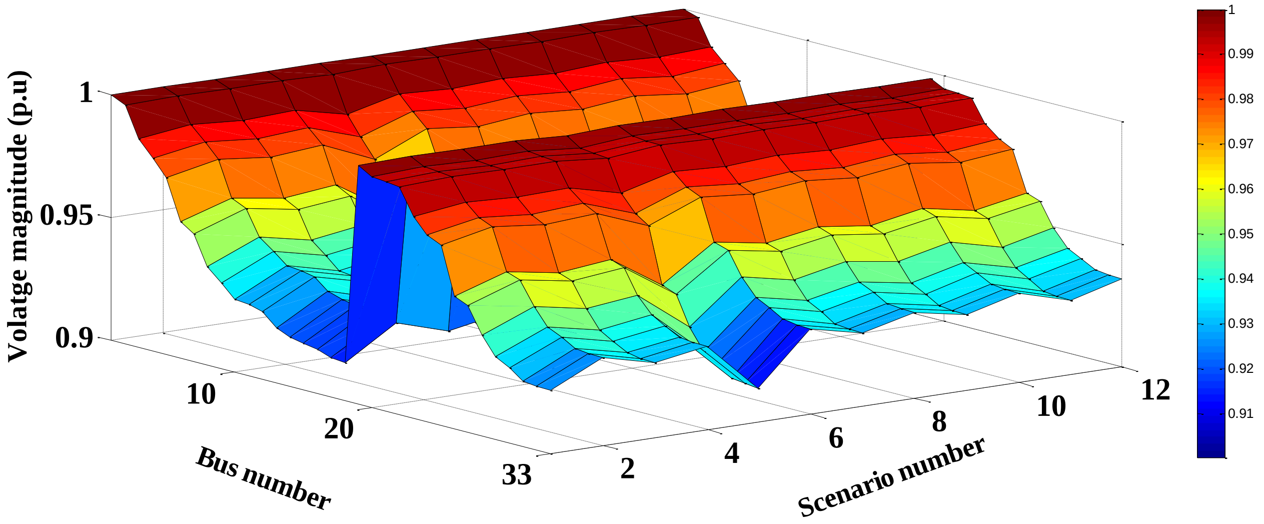

FIGURE 11. The voltage bus magnitudes for IEEE 33-bus network Without RDGs.

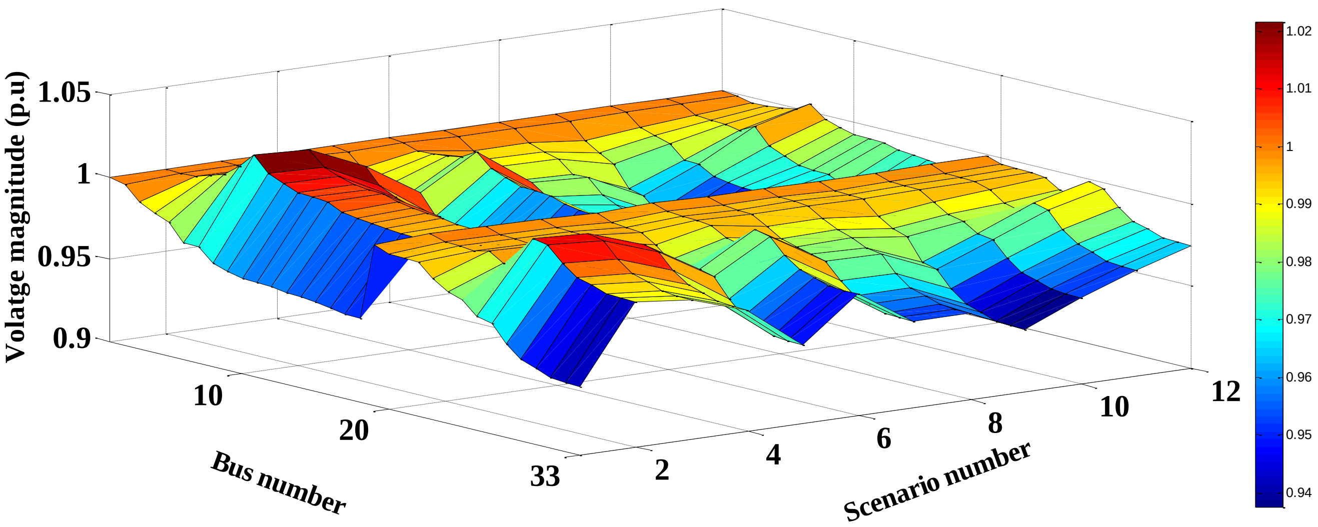

FIGURE 12. The voltage bus magnitudes for IEEE 33-bus network With RDGs.

5.2. 94-BUS System

In this section, AHA is used to find the optimal RDGs sizing and siting in the 94-bus network. The results show that buses 28th and 69th are the optimal sites for PV / WT units, respectively. Distributed Generators sizes are 764kW and 3979 kW, respectively. Table 9 shows the status of the distribution network with and without the inclusion of DGs. Because of variances in RDG output powers and load demand, the numbers in Table 10 change in each case. Figures 13, 14, 15, and 16 show the values for costs, emissions, VDs, and VSIs for each scenario with and without RDG integration, respectively. The voltage profiles of the 94-bus system are shown in Figures 17 and 18 for each condition. It is noted that RDGs can improve the voltage profile in any case. The outputs of the objective function utilizing several optimization algorithms are shown in table 11, and the AHA is superior to the PSO, WOA, SCA, and ALO strategies for solving this problem.

Table 9. The 95-bus system Simulation Results.

Item	Without RDGs	With RDGs	Percentage
Cost	344.3707	207.9793	39.6%
Emmissin	7345400	2747600	62.9%
VD	7.2416	1.5555	78.52 %
VSI	67.7145	88.2142	23.24 %

Table 10. The simulation results of 94-bus system.

Scenario	π_S	Loading %	$P_w(kW)$	$P_s(kW)$	$ETCost$(USD /h)	$ETEmission$ (kg/MWh)	$ETVD$(pu)	$ETVSI$(pu)
S1	0.001	84.25477	512.4	447.2835	0.378	6600	0.0054	0.0734
S2	0.009	66.14756	2813	54.3094	1.1275	7500	0.0091	0.8699
S3	0.13	75.2173	2785.3	214.6553	20.2787	188900	0.1216	12.463
S4	0.485	69.55373	2135.6	0	97.7351	1266500	0.5831	43.0353
S5	0.002	104.46	1634.6	149.1113	0.8005	13800	0.008	0.1563
S6	0.149	67.81934	1973.8	155.7095	28.8099	362100	0.1742	13.215
S7	0.005	76.93514	893.9	411.8605	1.5478	25300	0.0199	0.3911
S8	0.062	67.83325	860.9	98.0349	18.4141	302700	0.2641	4.7902
S9	0.017	75.22243	125.3	339.9435	6.4822	115000	0.1072	1.1991
S10	0.001	64.98827	512.2	483.5958	0.2812	4500	0.0043	0.0772
S11	0.091	75.91118	1713.3	125.2970	23.3654	349700	0.207	7.6712
S12	0.048	65.94618	1873.9	278.1169	8.7589	105000	0.0516	4.2725
Summation	**1**				**207.9793**	**2747600**	**1.5555**	**88.2142**

Table 11. The outcomes of using multiple Optimization techniques in the 94-bus system.

Optimizer	Average Values	Best Values	Worst Values	SD Values
AHA	**0.6277**	**0.6128**	**0.6564**	**0.0296**
PSO	0.6891	0.6522	0.7203	0.0235
ALO	0.6928	0.6613	0.7328	0.0582
WOA	0.6415	0.6229	0.6804	0.0180
SCA	0.6516	0.6185	0.6910	0.0200

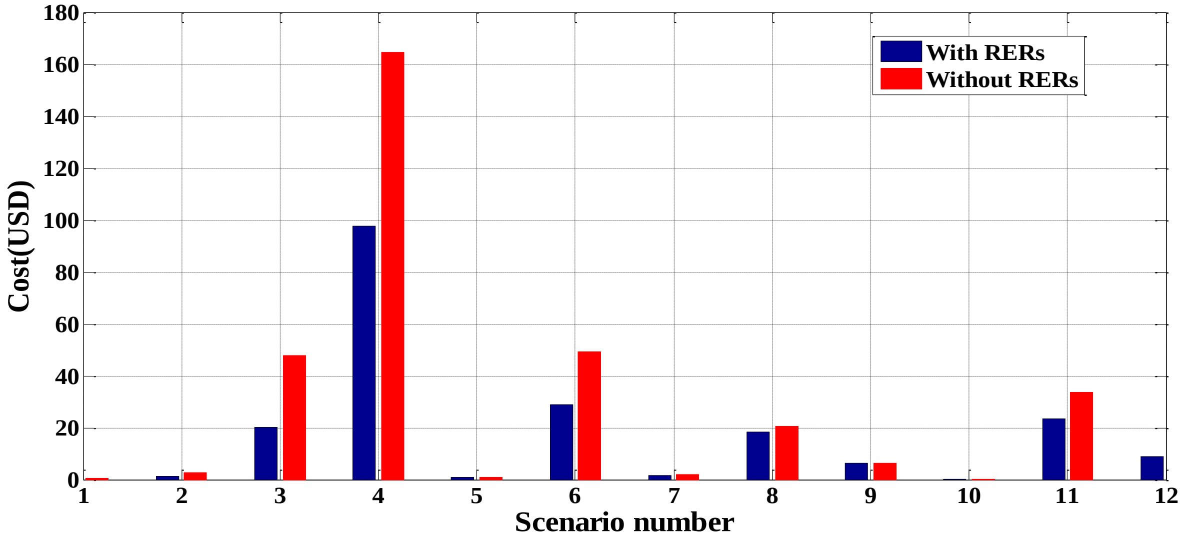

Figure 13. The total costs of 94-bus network.

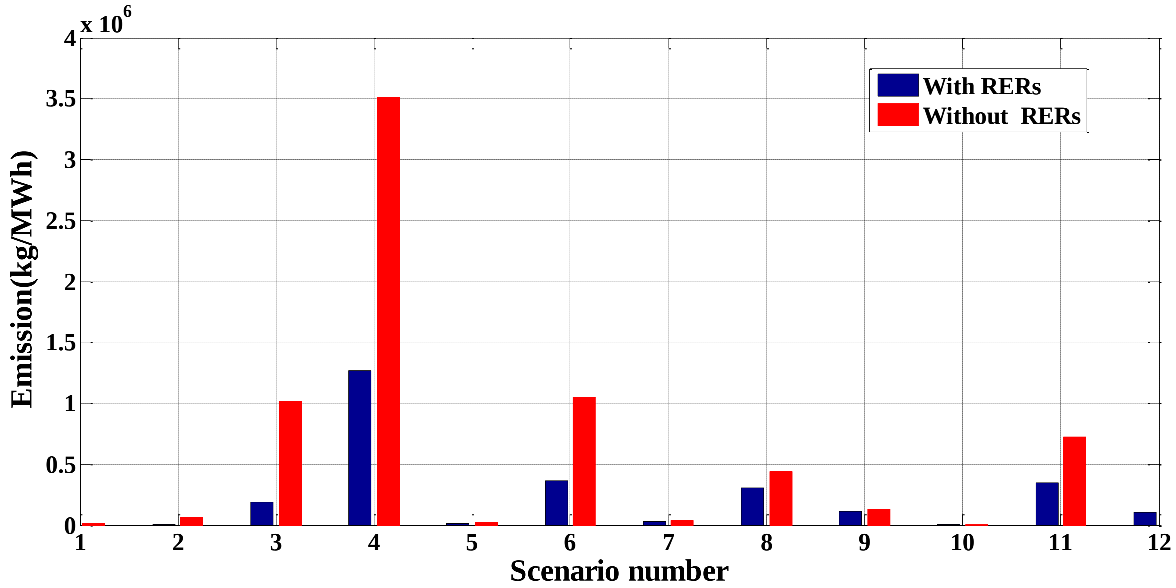

Figure 14. The total emissions of 94-bus network.

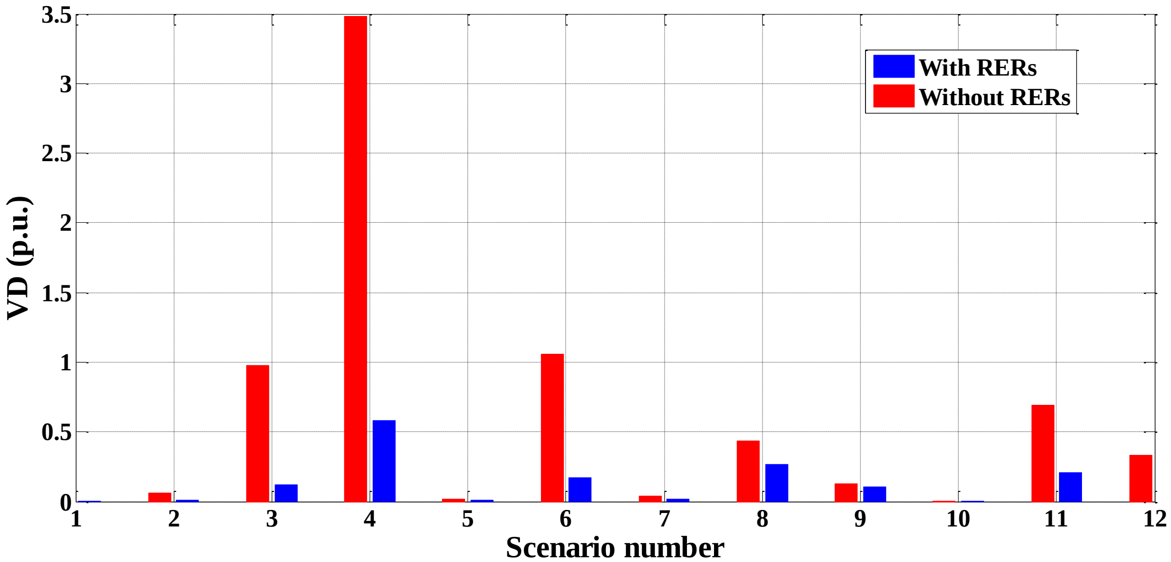

Figure 15. The total voltage deviation of 94-bus network.

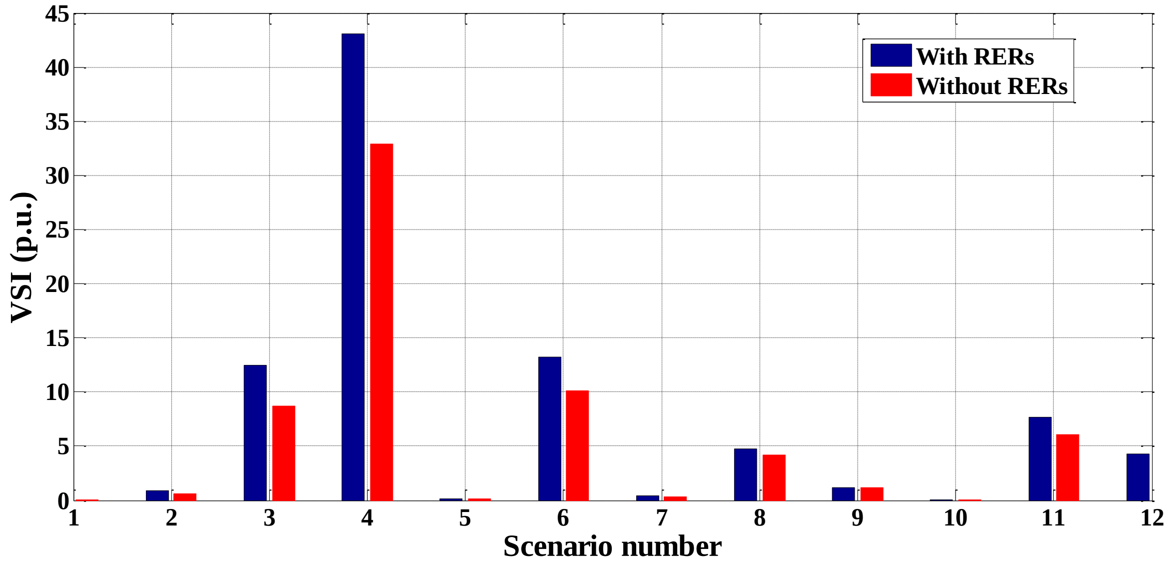

Figure 16. The total voltage stability index of 94-bus network.

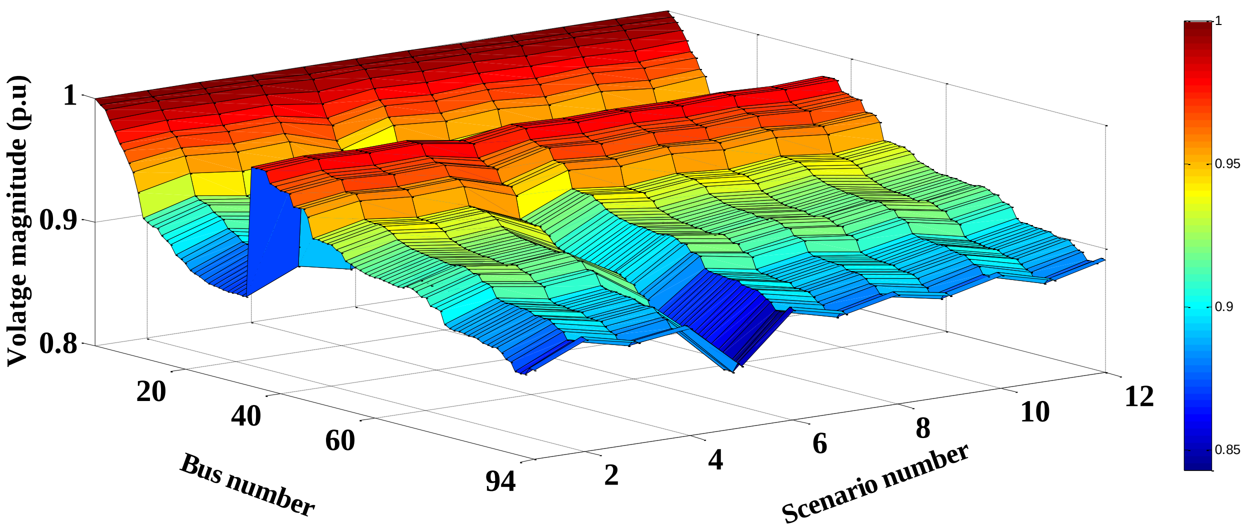

FIGURE 17. The 94-bus network voltage bus magnitudes, Without RDGs.

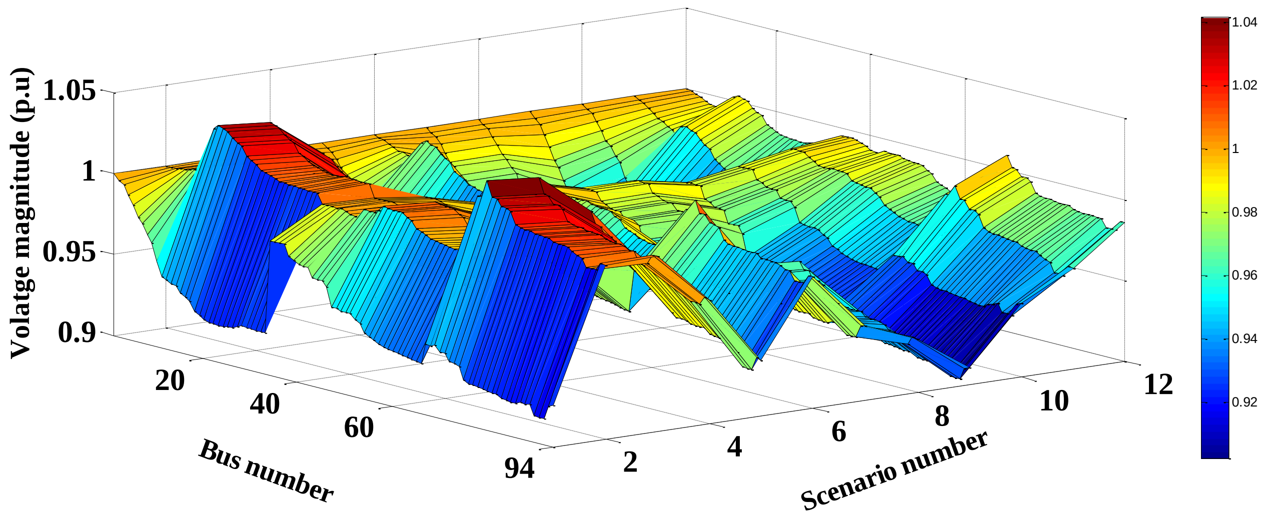

FIGURE 18. The 94-bus network voltage bus magnitudes, With RDGs.

6. CONCLUSION

The Artificial Hummingbird Algorithm (AHA) was introduced in this study as the most recent and efficient optimizer to determine the optimal sizing and siting of RDGs in RDN for a multi-objective function that includes decreasing total voltage deviations, emissions, costs, and increasing system stability. Solving the allocation problem of RDGs with and without considering the uncertainty of solar irradiance, loads, and wind speed has been presented in two different cases. The lognormal, and normal, Weibull PDFs for representing the uncertainties of PV solar irradiance, the loading, and the WT speed have been applied. Monte Carlo Simulation was utilized to create a series of scenarios. The large number of created scenarios was then limited to 12 scenarios using the backward reduction method. The allocation problem has been solved for two radial distribution networks including the IEEE 33-bus and 94-bus distribution system. The with and without conditions are compared and the results are enhanced by 38.91%, 62.43%, 70.48% and 12.12% for the IEEE 33-bus network. And by 39.6%, 62.59%, 78.52% and 23.24% for the 94-bus network. The computational study verified the superiority of the proposed algorithm over the WOA, ALO, PSO, and SCA techniques for solving the allocation problem.

Conflicts of Interest: The authors declare no conflict of interest.

References

[1] A. S. M. Ibrahim, "Optimal distributed generation allocation considering uncertainty of power generation and time-varying load," Universidad de Jaén, 2021.

[2] L. D. Pereira, I. Yahyaoui, R. Fiorotti, L. S. de Menezes, J. F. Fardin, H. R. Rocha, *et al.*, "Optimal allocation of distributed generation and capacitor banks using probabilistic generation models with correlations," *Applied Energy*, p. 118097, 2021.

[3] S. Chakraborty, S. Verma, A. Salgotra, R. M. Elavarasan, D. Elangovan, and L. Mihet-Popa, "Solar-Based DG Allocation Using Harris Hawks Optimization While Considering Practical Aspects," *Energies,* vol. 14, p. 5206, 2021.

[4] K. Sandhya and K. Chatterjee, "A review on the state of the art of proliferating abilities of distributed generation deployment for achieving resilient distribution system," *Journal of Cleaner Production*, vol. 287, p. 125023, 2021.

[5] D. Bogdanov, M. Ram, A. Aghahosseini, A. Gulagi, A. S. Oyewo, M. Child, *et al.*, "Low-cost renewable electricity as the key driver of the global energy transition towards sustainability," *Energy,* vol. 227, p. 120467, 2021.

[6] M. G. Hemeida, S. Alkhalaf, T. Senjyu, A. Ibrahim, M. Ahmed, and A. M. Bahaa-Eldin, "Optimal probabilistic location of DGs using Monte Carlo simulation based different bio-inspired algorithms," *Ain Shams Engineering Journal*, 2021.

[7] S. Lv, J. Li, Y. Guo, and Z. Shi, "A typical distributed generation scenario reduction method based on an improved clustering algorithm," *Applied Sciences,* vol. 9, p. 4262, 2019.

[8] S. S. Kola, "A review on optimal allocation and sizing techniques for DG in distribution systems," *International Journal of Renewable Energy Research (IJRER),* vol. 8, pp. 1236-1256, 2018.

[9] A. Ahmed, M. F. Nadeem, A. T. Kiani, and I. Khan, "An Overview on Optimal Planning of Distributed Generation in Distribution system and Key Issues," in *2021 IEEE Texas Power and Energy Conference (TPEC)*, 2021, pp. 1-6.

[10] M.-A. Hamidan and F. Borousan, "Optimal planning of distributed generation and battery energy storage systems simultaneously in distribution networks for loss reduction and reliability improvement," *Journal of Energy Storage,* vol. 46, p. 103844, 2022.

[11] S. Rudresha, S. G. Ankaliki, and T. Ananthapadmanabha, "Voltage stability analysis and loss minimization with integration of different types of DGs into the distribution system," *IJSDR,* vol. 4, pp. 185-189, 2019.

[12] S. Rudresha, S. G. Ankaliki, T. Ananthapadmanabha, and V. Girish, "Integration of Solar Photovoltaic Generation in a Practical Distribution System for Loss Minimization and Voltage Stability Improvement," in *Advances in Renewable Energy and Electric Vehicles*, ed: Springer, 2022, pp. 237-246.

[13] N. Mansouri, A. Lashab, J. M. Guerrero, and A. Cherif, "Photovoltaic power plants in electrical distribution networks: a review on their impact and solutions," *IET Renewable Power Generation,* vol. 14, pp. 2114-2125, 2020.

[14] J. Martins, S. Spataru, D. Sera, D.-I. Stroe, and A. Lashab, "Comparative study of ramp-rate control algorithms for PV with energy storage systems," *Energies,* vol. 12, p. 1342, 2019.

[15] N. Mansouri, A. Lashab, D. Sera, J. M. Guerrero, and A. Cherif, "Large photovoltaic power plants integration: A review of challenges and solutions," *Energies,* vol. 12, p. 3798, 2019.

[16] S. K. SUDABATTULA and K. MUNISWAMY, "Optimal Allocation of Different Types of Distributed Generators in Distribution System," *Gazi University Journal of Science,* vol. 32, pp. 186-203, 2019.

[17] P. Prakash and D. K. Khatod, "Optimal sizing and siting techniques for distributed generation in distribution systems: A review," *Renewable and sustainable energy reviews,* vol. 57, pp. 111-130, 2016.

[18] W. Zhao, L. Wang, and S. Mirjalili, "Artificial hummingbird algorithm: A new bio-inspired optimizer with its engineering applications," *Computer Methods in Applied Mechanics and Engineering,* vol. 388, p. 114194, 2022.

[19] A. A. Abou El-Ela, R. A. El-Sehiemy, and A. S. Abbas, "Optimal placement and sizing of distributed generation and capacitor banks in distribution systems using water cycle algorithm," *IEEE Systems Journal,* vol. 12, pp. 3629-3636, 2018.

[20] S. M. Mohseni-Bonab and A. Rabiee, “Optimal reactive power dispatch: A review, and a new stochastic voltage stability constrained multi-objective model at the presence of uncertain wind power generation,” *IET Gener. Transm. Distrib.*, vol. 11, no. 4, pp. 815–829, 2017, doi: 10.1049/iet-gtd.2016.1545.

[21] P. P. Biswas, P. N. Suganthan, and G. A. J. Amaratunga, “Optimal power flow solutions incorporating stochastic wind and solar power,” *Energy Convers. Manag.*, vol. 148, pp. 1194–1207, 2017, doi: 10.1016/j.enconman.2017.06.071.

[22] Soroudi, M. Aien, and M. Ehsan, “A probabilistic modeling of photo voltaic modules and wind power generation impact on distribution networks,” *IEEE Syst. J.*, vol. 6, no. 2, pp. 254–259, 2012, doi: 10.1109/JSYST.2011.2162994.

[23] P. P. Biswas, P. N. Suganthan, R. Mallipeddi, and G. A. Amaratunga, "Optimal reactive power dispatch with uncertainties in load demand and renewable energy sources adopting scenario-based approach," Applied Soft Computing, vol. 75, pp. 616-632, 2019.

[24] M. R. Elkadeem, M. Abd Elaziz, Z. Ullah, S. Wang, and S. W. Sharshir, "Optimal planning of renewable energy-integrated distribution system considering uncertainties," IEEE Access, vol. 7, pp. 164887-164907, 2019.

[25] A. Ramadan, M. Ebeed, S. Kamel, A. Y. Abdelaziz, and H. Haes Alhelou, "Scenario-Based Stochastic Framework for Optimal Planning of Distribution Systems Including Renewable-Based DG Units," Sustainability, vol. 13, p. 3566, 2021.